Tissue-Engineered Bone Immobilized with Human Adipose Stem Cells-Derived Exosomes Promotes Bone Regeneration

Wenyue Li,[†,‡] Yunsong Liu,[†,‡] Ping Zhang,[†,‡] Yiman Tang,[†,‡] Miao Zhou,[§] Weiran Jiang,[†,‡] Xiao Zhang,*[,†,‡] Gang Wu,*[,∥] and Yongsheng Zhou*[,†,‡]

[†]Department of Prosthodontics and [‡]National Engineering Lab for Digital and Material Technology of Stomatology, National Clinical Research Center for Oral Diseases, Beijing Key Laboratory of Digital Stomatology, Peking University School and Hospital of Stomatology, Beijing 100081, China

[§]Key laboratory of Oral Medicine, Guangzhou Institute of Oral Disease, Stomatology Hospital of Guangzhou Medical University, Guangzhou 510140, China

[∥]Department of Oral Implantology and Prosthetic Dentistry, Academic Centre for Dentistry Amsterdam (ACTA), Universiteit van Amsterdam and Vrije Universiteit Amsterdam, Amsterdam 1081 LA, The Netherlands

S *Supporting Information*

ABSTRACT: Exosomes, nanoscale extracellular vesicles functioning as cell-to-cell communicators, are an emerging promising therapeutic in the field of bone tissue engineering. Here, we report the construction and evaluation of a novel cell-free tissue-engineered bone that successfully accelerated the restoration of critical-sized mouse calvarial defects through combining exosomes derived from human adipose-derived stem cells (hASCs) with poly(lactic-*co*-glycolic acid) (PLGA) scaffolds. The exosomes were immobilized on the polydopamine-coating PLGA (PLGA/pDA) scaffolds under mild chemical conditions. Specifically, we investigated the effects of hASC-derived exosomes on the osteogenic, proliferation, and migration capabilities of human bone marrow-derived mesenchymal stem cells in vitro and optimized their osteoinductive effects through osteogenic induction. Furthermore, an in vitro assay showed exosomes could release from PLGA/pDA scaffold slowly and consistently and in vivo results showed this cell-free system enhanced bone regeneration significantly, at least partially through its osteoinductive effects and capacities of promoting mesenchymal stem cells migration and homing in the newly formed bone tissue. Therefore, overall results demonstrated that our novel cell-free system comprised of hASC-derived exosomes and PLGA/pDA scaffold provides a new therapeutic paradigm for bone tissue engineering and showed promising potential in repairing bone defects.

KEYWORDS: exosomes, human adipose-derived stem cells (hASCs), osteogenesis, cell-free therapy, bone tissue engineering
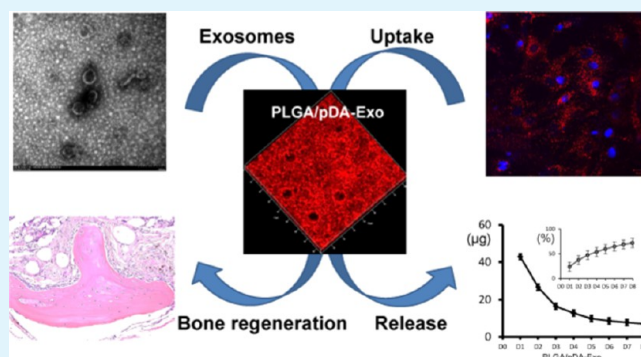
INTRODUCTION

Large-sized bone defects can severely compromise esthetics and musculoskeletal functions of patients. Mesenchymal stem cells (MSCs)-based bone tissue engineering has been valued as a promising strategy in this field.[1] Numerous studies have demonstrated that the MSC-based tissue-engineered bone (TEB) could efficaciously restore the critical-sized bone defects and accelerate bone regeneration.[2,3] Over the years, cell delivery has been used as the classical approach in the cell-based therapy.[4,5] However, the direct use of MSCs has several notable limitations, such as a time-consuming cell culture process, phenotype changes of MSCs during cell expansion, low homing efficiency of the injected cells, and a low survival rate of local transplanted cells.[6,7] Therefore, various alternative techniques have been developed to avoid the limitations of direct cell transplantation. In addition, recent evidence also indicated that the therapeutic effects of MSCs were largely

facilitated via the paracrine mechanism to stimulate the activity of tissue-resident recipient cells, instead of direct cell replacement.[8] This paradigm shift was supported by the studies demonstrating that either conditioned culture medium or extracellular vesicles (EVs) showed similar therapeutic effects with MSCs in diverse animal models.[9,10]

Exosome-based cell-free therapy appears to be a promising strategy for the restoration of bone defects. Exosomes are nanovesicles that could be constitutively released by plasma membrane fusion, with the responsibility of mediating local and systemic cell−cell communication through the transfer of mRNAs, miRNAs, and proteins.[9−13] Recent studies have demonstrated that exosomes play pivotal roles in various

physiological or pathological activities, such as immunomodulation, tumorigenesis, angiogenesis, and wound healing.[14−17] Hitherto, MSCs seem to be the most prolific producers of exosomes.[18] MSC-derived exosomes delivered bioactive molecules to recipient cells and mimicked the therapeutic effects of MSCs.[19−21] In comparison with direct cell transplantation, exosome-based therapy has advantages, such as high stability, intrinsic homing effect, low immunogenicity, and the lack of unwanted cell accumulation in liver.[22]

The basis of exosome-related therapies lies in sufficient parent cell sources for exosomes' production. Among the different sources of MSCs, adipose tissue has been considered as an abundant and accessible pool for the benefits of wide distribution in human body and less invasive and expensive extraction procedures.[23] Our previous studies have demonstrated that human adipose-derived stem cells (hASCs) can undergo rapid and efficient osteogenic differentiation both in vitro and in vivo.[24] Moreover, recent studies showed that hASC-derived exosomes could exert the similar biological effects of hASCs and play important roles in angiogenesis and wound healing.[14,25] However, the effects of hASC-derived exosomes on bone regeneration remains to be unveiled. Therefore, in this study, we aim to optimize and investigate the osteoinductive effects of hASC-derived exosomes in vitro and in vivo.

To exert the optimal biological efficacy of exosomes, we mimic the paracrine function of cells by a slow-release system. Poly(lactic-co-glycolic acid) (PLGA) has been used widely in tissue engineering due to its appropriate mechanical strength and biodegradation properties.[26] However, like most of the synthetic organic materials, the limited bioactivity to induce and enhance bone regeneration made it far from an ideal material in bone engineering. Compared with regular physical adsorption methods, a mussel-inspired immobilization strategy assisted by polydopamine (pDA) provided a more efficient factor coating on PLGA substrates.[27] In our previous studies, we modified the PLGA scaffolds through polydopamine (pDA)-mediated immobilization of bone forming peptide-1 (BFP-1). An in vitro assay indicated PLGA/pDA-BFP-1 scaffolds released BFP-1 slowly, and the in vivo experiment showed that the combination of hASCs and PLGA/pDA-BFP-1 significantly enhanced bone formation in nude mice.[28] In this study, we elaborately constructed a cell-free bone tissue engineering system by combining the PLGA/pDA scaffold with exosomes.

The purpose of this study was therefore to unveil the biofunctions of hASC-derived exosomes on osteogenesis in vitro and in vivo and construct a novel exosome-based TEB.

■ EXPERIMENTAL SECTION

Cell Culture. Primary hASCs and human bone marrow-derived mesenchymal stem cells (hBMSCs) were purchased from ScienCell Company (San Diego, CA). Cells were expanded in proliferation medium (PM) containing Dulbecco's modified Eagle's medium (Gibco, Grand Island, NY), 10% (v/v) fetal bovine serum (FBS) (ScienCell), 100 U/mL penicillin G, and 100 mg/mL streptomycin (Gibco) at 37 °C in an incubator with 5% CO_2 atmosphere and 100% relative humidity. All in vitro experiments were repeated three times using cells from three donors, respectively. To induce osteogenic differentiation, MSCs were cultured in osteogenic medium (OM) containing 100 nM dexamethasone, 10 mM β-glycerophosphate, and 0.2 mM ascorbic acid. All other materials were purchased from Sigma-Aldrich (St. Louis, MO) unless otherwise stated.

Isolation, Purification, and Identification of Exosomes. Exosomes were isolated from conditioned medium of hASCs in

vitro. FBS in medium was ultracentrifugated for 12 h at 100 000g for bovine exosomes depletion before use. Several centrifugation and filtration steps were performed for exosomes purification according to previous studies.[29,30] Briefly, the supernatant was centrifuged at 2000g for 20 min, to eliminate cells, and 10 000g for 40 min, followed by a 0.22 μm filter filtration to eliminate cellular debris. Then, the supernatant was ultracentrifuged at 100 000g for 70 min and additionally washed with phosphate-buffered saline (PBS) at 100 000g for 70 min (Ultracentrifuge, Beckman Coulter, L-90K).

Transmission electron microscopy (TEM) was utilized to observe the morphology of exosomes. Concentrated exosomes from hASCs were fixed with 2% paraformaldehyde for 30 min; then, the mixture (about 8 μL) was dropped onto carbon-coated copper grids and air-dried for 10 min, then stained with 1% uranyl acetate two times (6 min each). Images were obtained using an HT7700 TEM (Hitachi, Japan) at 120 kV.[31]

Nanoparticle tracking analysis (NTA) was used to identify the particle size/concentration and particle size distribution. Exosomes were recorded according to the manufacturer's instructions (Nanosight LM10 system, Amesbury, U.K.), and the results were analyzed with NTA analytical software (Nanoparticle Tracking Analysis, version 2.3).

In addition, western blotting was performed to identify the exosomal markers. The protein content was determined using bicinchoninic acid protein assay kit (Thermo Fisher Scientific, Rockford, IL). Equal amounts of proteins were prepared for cells and exosomes lysed with ice-cold radio immunoprecipitation assay buffer containing protease inhibitor cocktail. Exosomes were confirmed to express protein CD63 (abcam) and CD9 (abcam), whereas in the absence of Tubulin (cytosolic marker) (Santa Cruz Biotechnology, Inc.) and Histone 1 (nuclear marker) (Santa Cruz Biotechnology, Inc.) they were confirmed by Western blotting.[32] Cell extract was used as control.

Exosomes Uptake Assay. Exosomes were labeled with PKH-26 (Sigma-Aldrich) to determine their uptake by hBMSCs.[29] According to the manufacturer's protocol, exosomes diluted in 1 mL of Diluent C and 4 μL of PKH-26 dye diluted in 1 mL of Diluent C were incubated together. After 4 min, 2 mL of 0.5% bovine serum albumin/PBS was added to bind excess dye. Then, labeled exosomes were washed in PBS at 100 000g for 1 h. Thereafter, the exosome pellet was incubated with hBMSCs for 2, 24, 48, and 72 h, respectively. After the incubation, the cells were washed twice with PBS, then fixed in 4% paraformaldehyde for 10 min and washed again. 6-Diamidino-2-phenylindole (DAPI) solution was used for the staining of nuclei. Images were captured with a LSM 5 EXCITER confocal imaging system (Carl Zeiss, Oberkochen, Germany).

Determination of Optimal Exosomes. To determine the optimal time point and concentration for isolated hASC-derived exosomes, exosomes were isolated from supernatants of hASCs after 0, 2, 4, 7, and 14 days of osteoinduction by OM. Meanwhile, Pierce (Thermo Fisher Scientific, Rockford, IL) protein assay kit was used to determine the concentration of exosomes. To identify the osteoinductive effects of exosomes on MSCs, the hBMSCs were exposed to different treatments. After 7 days of induction, alkaline phosphatase (ALP) activity assays were performed. ALP staining was performed, as described in detail previously.[24] Meanwhile, ALP activity was determined using an ALP kit according to the manufacturer's protocol and normalized to the total protein content, as previously described.[24]

Proliferation, Migration, and Osteogenic Differentiation of hBMSCs Stimulated by Exosomes in Vitro. *Experimental Design.* On the basis of the results of the "Determination of Optimal Exosomes", 25 μg/mL exosomes, which were isolated from the supernatant of hASCs after 2 days of osteoinduction, were selected as the optimal concentration in in vitro experiments. The hBMSCs were exposed to the following treatments: (1) negative control medium (PM); (2) PM with 25 μg/mL exosomes; (3) positive control medium (OM); (4) OM with 25 μg/mL exosomes.

Cell Proliferation and Migration Assay. For cell proliferation assays, the cell number was evaluated using cell-counting kit-8 (CCK-

Table 1. List of Primers Used in This Study for Real-Time PCR

gene	forward (5′−3′)	reverse (5′−3′)
β-actin	CATGTACGTTGCTATCCAGGC	CTCCTTAATGTCACGCACGAT
RUNX2	ACTACCAGCCACCGAGACCA	ACTGCTTGCAGCCTTAAATGACTCT
ALP	ATGGGATGGGTGTCTCCACA	CCACGAAGGGGAACTTGTC
COL1A1	ACAGGGCTCTAATGATGTTGA	AGGCGTGATGGCTTATTTGT
OCN	CACTCCTCGCCCTATTGGC	CCCTCCTGCTTGGACACAAAG

8) according to the manufacturer's instructions (Dojindo Laboratories, Kumamoto, Japan) and growth curves were drawn with the absorbance values ($n = 6$).

The migration of hBMSCs was evaluated by transwell assays. Briefly, 1×10^5 cells were loaded into the upper compartment of a transwell chamber with 8 μm pore filters (Corning) and 500 μL of medium with or without exosomes were added to the lower compartment. After culturing for 24 h, the chamber was gently washed by PBS. To remove the nonmigrated cells, the upper side of the membrane was wiped with a cotton swab. Then, the membranes were fixed with 4% paraformaldehyde and stained with 0.5% crystal violet for 10 min. The number of migrated cells was counted in five randomly selected microscopic fields per filter.

Cell Differentiation Assays. The hBMSCs were seeded in 12-well plates and divided into four groups, as above. The ALP activity assay was performed as described in Determination of Optimal Exosomes section above.

To assess the mineralization, alizarin red staining was performed on day 14 after osteoinduction. Cells were washed three times with phosphate-buffered saline (PBS), fixed with ethanol for 30 min, and then stained with 1% alizarin red S staining solution (pH 4.2, Sigma-Aldrich) at room temperature. To quantitatively determine matrix calcification, alizarin red was destained with 10% cetylpyridinium chloride in 10 mM sodium phosphate for 30 min and evaluated by absorbance values at 562 nm. The final mineralization levels in each group were normalized to the total protein concentrations obtained from duplicate plates.[24]

Real-Time Quantitative Polymerase Chain Reaction (qPCR) Analysis. The total RNA were isolated with TRIzol reagent (Invitrogen) at 7 and 14 days after osteoinduction; then, only those RNA with optical density ratios (Nano Drop 8000, Pierce Thermo Scientific) of 1.8−2.0 (260/280 nm) were reverse-transcribed to cDNA (Takara, Tokyo, Japan; #RR037A). Real-time PCR was conducted using a 7500 Real-Time PCR Detection System (Applied Biosystems, Foster City, CA) with SYBR Green Master Mix (Roche Applied Science, Mannheim, Germany). The primers for runt-related transcription factor 2 (RUNX2), alkaline phosphatase (ALP), collagen type I alpha 1 (COL1A1), and osteocalcin (OCN) are listed in Table 1. β-actin was used for normalization.

Construction of Novel Cell-Free Tissue-Engineered Bone (TEB) Comprised of Exosomes and PLGA/pDA Scaffold. Cylindrical PLGA (lactide/glycolide: 50/50) of 4 mm diameter and 2 mm height were purchased from Shandong Academy of Pharmaceutical Sciences (Shandong, China). According to our previous study,[28] the scaffolds soaked in dopamine (DA) solution (2 mg/mL in 10 mM Tris-HCl, pH 8.5, Sigma-Aldrich, St. Louis, MO) were incubated with shaking at 37 °C for 18 h for the formation of pDA film. To remove the unattached DA molecules, the scaffolds were washed in an ultrasonic cleaner with distilled water until the water became clear. The scaffolds were sterilized in 75% ethanol for 1 h and then washed with sterilized PBS three times before the next step.

For the immobilization of exosomes, PLGA/pDA, or PLGA only, substrates were immersed in 1 μg/μL exosome solution (250 μL/scaffold) for 12 h at 4 °C. To observe the distribution of exosomes on the scaffold, the exosomes were labeled with PKH-26, as described above, and the images were captured with an LSM 5 EXCITER confocal imaging system (Carl Zeiss, Oberkochen, Germany) and the scaffolds were stained with PKH-26 as control. After exosomes' immobilization, the compound materials were incubated in saline at 37 °C (physiologically relevant conditions) and the supernatants were

collected at predetermined time intervals of 1−8 days to measure the exosomes' release. The amount of exosomes released was measured using the Pierce (Thermo Fisher Scientific, Rockford, IL) protein assay kit.

The surface morphology of the materials was observed by field emission scanning electron microscopy (SEM). After being washed with PBS, the samples were fixed in cacodylate buffered 4% glutaraldehyde for 12 h at 4 °C and dried in a Micro Modul YO-230 critical point dryer (Thermo Scientific, Waltham, MA). Then, the samples were mounted onto aluminum stubs, sputter-coated with gold, and viewed with a Hitachi S4800 instrument (Hitachi, Tokyo, Japan).

Animal Experiments. Five-week-old male BALB/C mice were used in animal experiments. All animal experiments were approved by the Peking University Animal Care and Use Committee and performed in accordance with the institutional animal guidelines. The mice were randomly divided into three groups with eight in each group: (1) PLGA scaffold only (PLGA group); (2) PLGA scaffold coated with pDA (PLGA/pDA group); (3) PLGA/pDA scaffold + exosomes (PLGA/pDA-Exo group). In situ skull defect experiment was performed as described previously.[6] Briefly, a 4 mm diameter critical-sized defect was made at the calvarium with a trephine bur (Hager Meisinger GmbH, Neuss, Germany) under low-speed drilling. Copious saline irrigation was necessary for lowering the temperature, and the operation had to be proceeded carefully to avoid damage to the dura mater and brain. The scaffolds were then implanted into the defects, and the incision was stitched.

Analysis of Bone Regeneration in Vivo. Specimens of each group were harvested at 6 weeks after implantation. Mice in each group were sacrificed by CO_2 inhalation. Thereafter, the whole calvaria including the implants was surgically removed and fixed in 4% paraformaldehyde. A high-resolution Inveon microcomputed tomography (CT) (Siemens, Munich, Germany) was used for scanning to show the bone formation within the bone defect. The thresholding of mineralized bone was set at 500. The gray value of PLGA material was around −329, as tested on our machine (with water at 0 and air at −1000). Therefore, PLGA was not included in the analysis of new bone volume. Multimodal three-dimensional (3D) visualization software (Inveon Research Workplace, Siemens, Germany) was used for 3D reconstruction of the images and evaluating new bone volume in the defects by quantifying pixels in these regions. Thereafter, the specimens were decalcified for 20 days in 10% ethylenediaminetetra-acetic acid (pH 7.4). After decalcification, the specimens were dehydrated and subsequently embedded in paraffin. Hematoxylin & eosin (HE) staining and Masson staining were performed. Bone regeneration in the defect regions was evaluated by immunohisto-chemical (IHC) analysis for RUNX2 and osteocalcin (OCN) (ab93876-Osteocalcin, ab23981-RUNX2, Abcam, Cambridge, U.K.).

Chemotactic Capability Exosomes in Vivo. Immunofluorescence staining of frozen sections with antibodies to stage-specific embryonic antigen-4 (SSEA-4) and CD45 was used to identify MSCs.[6,33] Immunofluorescence with FITC- and Texas Red-conjugated secondary antibodies (Cell Signaling Technology Inc) were used to visualize the antibody staining. Cell nuclei were stained with DAPI. Images were captured with a Leica microscope and imaged with a Charge-coupled device camera (Retiga EXi; Qimaging, Surrey, BC, Canada). The number of migrated SSEA-4+/CD45− cells was counted in five randomly selected microscopic fields.

Statistical Analysis. Data were analyzed using SPSS software (Chicago, IL). Comparisons between two groups were analyzed by independent two-tailed Student's t tests. Comparisons between more
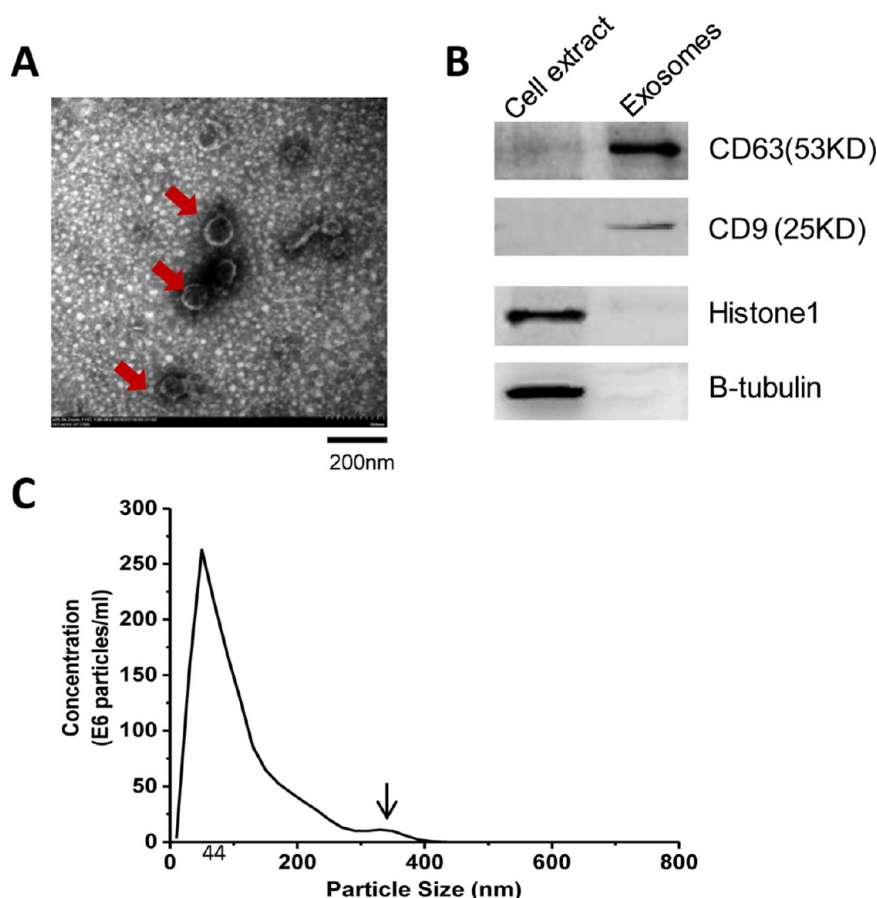
Figure 1. Characterization of exosomes derived from human adipose-derived stem cells (hASCs). (A) Morphology of exosomes observed by transmission electron microscopy. (B) Western blot analysis of the exosomal surface markers. (C) Particle size distribution of exosomes measured by NanoSight analysis: the mean size ± SD of exosomes was 105 ± 72 nm. The right peak in the graph (↓) indicated that exosomes clumped together during analysis.

than two groups were analyzed by one-way analysis of variance followed by a Tukey's post hoc test. The final results were expressed as the mean ± standard deviation (SD) of 3−10 experiments per group. For all tests, statistical significances were accepted for P values lower than 0.05.

RESULTS

Characterization of hASC-Derived Exosomes. TEM analysis showed that the exosomes isolated from the supernatants of hASCs bore a cup-shaped morphology (Figure 1A). NTA analysis indicated that the parameters of the exosomes ranged mainly from 33 to 177 nm (Figure 1C). Western blotting analysis (Figure 1B) showed that the exosome-specific markers CD63 and CD9 were detected in hASC-derived exosomes without the presence of either Tubulin (cytosolic marker) or Histone 1 (nuclear marker).

Internalization of Exosomes by hBMSCs. To investigate whether exosomes could enter into the cytoplasm of hBMSCs, we incubated the labeled exosomes with hBMSCs for 2, 24, 48, and 72 h, respectively. Fluorescence microscopy analysis (Figure 2) showed that the hASC-derived exosomes labeled PKH-26 (the red dots) were gradually internalized by the hBMSCs from 2 to 24 h. At 48 h post incubation, a large number of exosomes have been internalized and distributed in the perinuclear region. Then, at 72 h, the number of the red dots decreased, which may be due to the metabolism of the host cells.

Screening the Optimal Osteoinductive Property of Exosomes from hASCs with Different Time Spans of Osteogenic Induction. The osteogenic differentiation of hASCs was induced by OM for 14 days, which was confirmed by the significantly enhanced ALP staining (Figure S1A), ALP activity (Figure S1B), alizarin red staining (Figure S1C), and the mRNA expressions of osteogenic gene, such as *RUNX2* (Figure S1D) and *OCN* (Figure S1E) at 4, 7, or 14 days. We screened the osteoinductive activity of the exosomes isolated from hASCs at different time spans of osteogenic induction using ALP activity as an indicator. Our results showed that nonosteogenically induced hASC-derived exosomes (0d-Exo) were not able to significantly enhance the ALP activity of hBMSCs either in PM or in OM after culture for 7 days (Figure 3). The exosomes derived from osteogenically induced hASCs could significantly enhance ALP activity of hBMSCs in OM but not in PM, irrespective of the different time spans (2, 4, 7, and 14 days) of osteogenic induction. In OM, the ALP activity under stimulation by 25 μg/mL exosomes was significantly higher than that by 10 or 50 μg/mL exosomes (Figure 3). Consequently, we selected the 25 μg/mL exosomes derived from the hASCs that were osteogenically induced for 2 days in the following in vitro assays.

Effects of Exosomes on the Proliferation, Migration, and Osteogenic Differentiation of hBMSCs. The cell proliferation of hBMSCs increased with time within the 8 day monitoring span. In the first 2 days, no significant differences
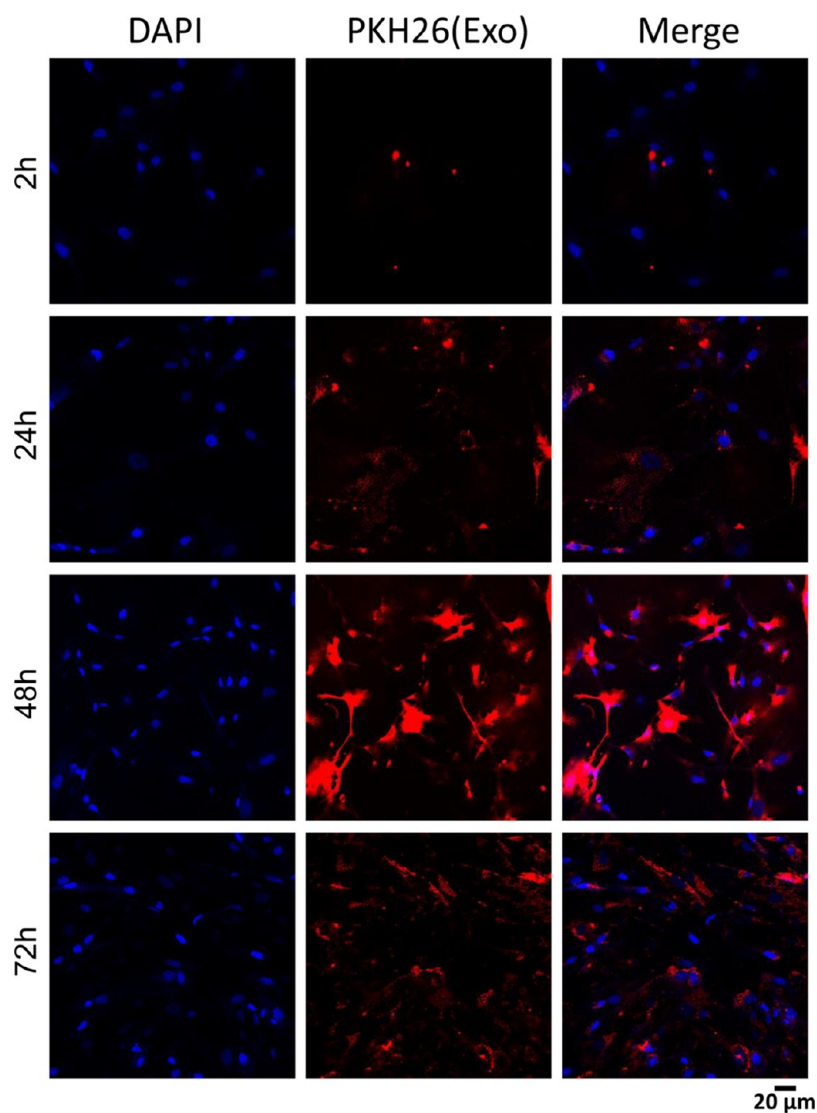
Figure 2. Cellular internalization of exosomes by human bone marrow-derived mesenchymal stem cells (hBMSCs). hBMSCs were incubated with PKH-26-labeled exosomes (red) for 2, 24, 48, and 72 h, respectively. The nucleus of hBMSCs was stained with DAPI (blue).

could be detected between the exosomes group and the control group. From the 3rd to the 8th day, the optical density value in the exosome-treated group was significantly higher than that in the control group (Figure 4A). In the migration assay, when the exosomes were added in the lower compartment, the number of cells migrating through the membrane was increased by approximately 3-folds than that in the control group both in PM and in OM (Figure 4B,C).

After the induction by hASC-derived exosomes for 7 and 14 days, ALP staining and ALP activity (Figure 5A,C) in the hBMSCs were significantly enhanced by the exosomes when cultured in OM but not in PM. Alizarin red staining and extracellular matrix mineralization assays (Figure 5B,D) demonstrated that cell matrix mineralization was significantly elevated after a 14 day induction by the exosomes in comparison to that of OM without exosomes. Consistently, the mRNA expression of a series of osteoblastogenesis-related genes (*RUNX2*, *ALP*, and *COL1A1*) in hBMSCs was also significantly upregulated when treated with OM + exosomes on day 7 and 14 compared to that of OM (Figure 5E).

Morphological Analysis and Release Kinetics of the Novel TEB in Vitro. After the process of pDA coating and

exosomes immobilization, the SEM picture confirmed the changes of surface morphology of the materials (Figure 6A). The exosome particles distributed on the surface of PLGA/pDA-Exo scaffold exhibited a cup-shaped and refractive morphology, which differed from that of the polydopamine particles on the surface of PLGA/pDA scaffold. The laser confocal scanning microscopic images showed that the PKH-26-labeled exosomes (red dots) homogeneously distributed on the surface of the scaffolds after the immobilization process, whereas there were only scattered irregular patches on the scaffold when stained with PKH-26 as control. More red dots were observed on the PLGA/pDA scaffold compared to that in the PLGA-only scaffold (Figure 6B). The total amount of grafted exosomes was 165.72 ± 15.4 μg on each PLGA/pDA scaffold and 73.6 ± 22.4 μg on each PLGA scaffold. The incorporated exosomes showed burst release from the PLGA scaffolds (left graph in Figure 6C), and almost all exosomes were depleted within 4 days. In contrast, exosomes showed a slow-release profile from the PLGA/pDA-Exo scaffold during the 8 day monitoring span, with about $28.19 \pm 9.2\%$ of the immobilized exosomes still maintained on the scaffold after 8 days (Figure 6C).
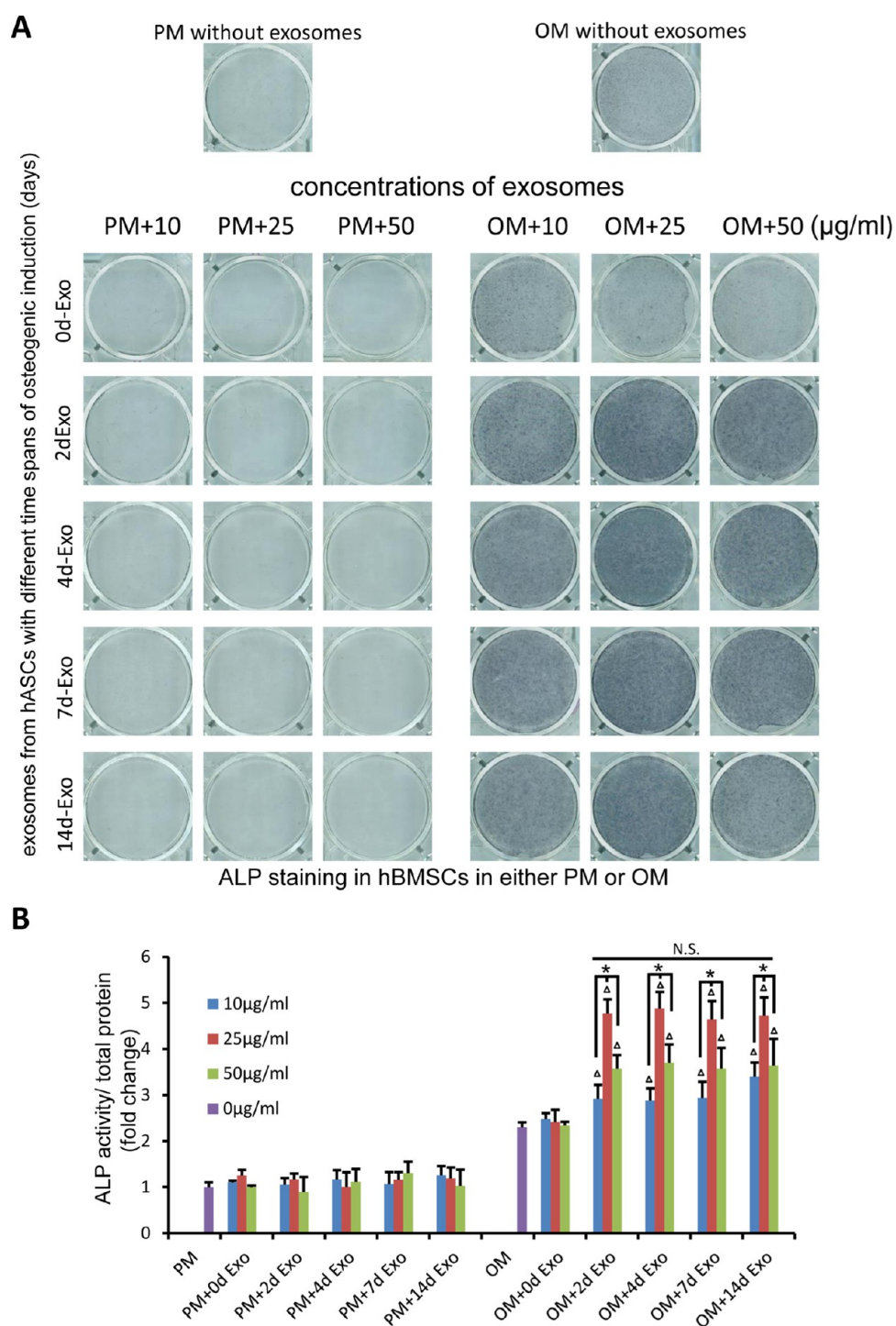
Figure 3. Alkaline phosphatase (ALP) assays of hBMSCs cultured for 7 days after osteoinduction to determine the optimal time point and concentration for exosomes. (A) ALP staining of hBMSCs after incubation with exosomes (10, 25, and 50 μg/mL) from hASCs after 0, 2, 4, 7, 14 days of osteoinduction. (B) ALP activity normalized against the total protein content. PM: proliferation medium; OM: osteogenic medium; *$p < 0.05$ versus the groups treated with exosomes on the same day after osteoinduction; $^{\triangle}p < 0.05$ versus the OM; N.S., not significant.

Micro-CT Analysis and Histological Assessment of Bone Regeneration in Critical-Sized Mouse Calvarial Defects in Vivo.

Micro-CT images revealed an almost complete lack of healing in the defects of the PLGA group, whereas in the PLGA/pDA group, a small number of high-density spots were observed. In contrast, several high-density spots and small peninsulas of bone nodule formation along the margins of bone defect could be observed in the group of PLGA/pDA-Exo (Figure 7A). Quantification of micro-CT images (Figure 7B) provided further evidence that significantly more new bone was formed in the PLGA/pDA-Exo group than in the other two groups.

HE staining of representative sections from the three groups indicated that the bone defects of the PLGA group and PLGA/pDA group were mainly filled with fibrotic connective tissues. In contrast, newly formed bone tissue was observed both along the border and in the center of the defects in the PLGA/pDA-Exo group (Figure 7C). Masson staining showed that more
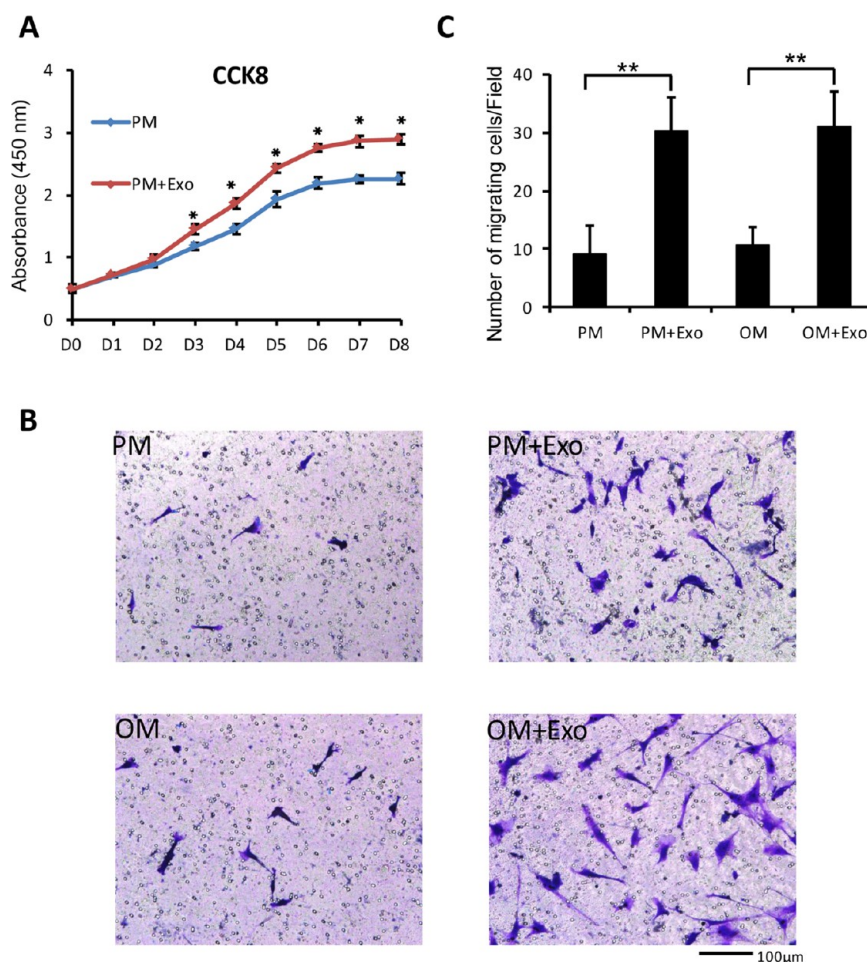
Figure 4. Human adipose-derived stem cell (hASC)-derived exosomes enhanced the proliferation and migration of human bone marrow-derived mesenchymal stem cells (hBMSCs). (A) Growth curves, measured using a CCK-8 kit; (B, C). The exosomes had a positive effect on the migration capacity of hBMSCs in transwell assays whether in PM or OM condition. PM: proliferation medium; OM: osteogenic medium; *$p < 0.05$ compared with the control group. **$p < 0.01$ compared with the group without exosomes.

mature collagen formations were present in the PLGA/pDA-Exo group compared to those in the PLGA/pDA and PLGA group (Figure 7D). The IHC staining showed that the exosomes' participation was associated with more cells that were positively stained with RUNX2 and OCN, the two key osteogenic markers (Figure 7E,F).

Effect of Exosomes on Recruitment of Host MSCs in Vivo. SSEA-4 (green)-positive and CD45 (red)-negative cells were considered to be MSCs.[6] MSCs were indicated by white arrows in the histological sections with immunofluorescence staining (Figure 8A). The engraftment of MSCs in scaffolds of PLGA/pDA-Exo group was significantly higher compared to that of the PLGA/pDA group (Figure 8B).

DISCUSSION

Bone tissue engineering is an interdisciplinary technology that elaborately combines cells, materials, and biochemical/physicochemical factors to improve or replace biological tissues.[34] Apart from the traditional bone tissue engineering technologies, e.g., cell-, gene-, and growth factor-based therapies, MSC-derived exosome-based therapy is a recently emerged and promising technique for bone tissue engineering.[35−37] Our goal is to develop a clinically applicable and efficacious exosome-based TEB to repair bone defects. In this study, we first showed that 25 μg/mL exosomes derived from hASCs that were

osteogenically induced for 2 days bore the most efficacious osteoinductive activity. Thereafter, we showed that the TEB elaborately combining a pDA−PLGA scaffold with the exosomes could significantly promote the osteogenesis in a critical-sized bone defect. Consequently, the novel TEB of PLGA/pDA-Exo showed a very promising application potential for bone tissue engineering.

An ideal parent cell type for yielding suitable exosomes for bone tissue engineering and clinical application should be safe, easy to obtain, available in large quantity, efficient in yielding, and adaptable to the increase of osteoinductivity of exosomes. In line with these requirements, many cells, such as dendritic cells, mast cells, epithelial cells, and tumor cells,[38] are not suitable parent cells for this application. MSCs, the most frequently used cell type in cell-based tissue engineering, have been widely accepted as promising parent cells for yielding exosomes. A noninvasive way to achieve MSCs is to differentiate induced pluripotent stem cells (iPSCs).[39,40] The exosomes derived from iPSC-MSCs (iPSC-MSC-Exosomes) have been shown to significantly promote the in vitro osteoblastogenesis of BMSCs and the in vivo angiogenic and osteogenic activities.[41] Furthermore, the potent angiogenic activity of iPSC-MSC-Exosomes could attenuate limb ischemia[42] and prevent osteonecrosis[43] in mice. On the other hand, although iPSC-MSCs have already been investigated for bone
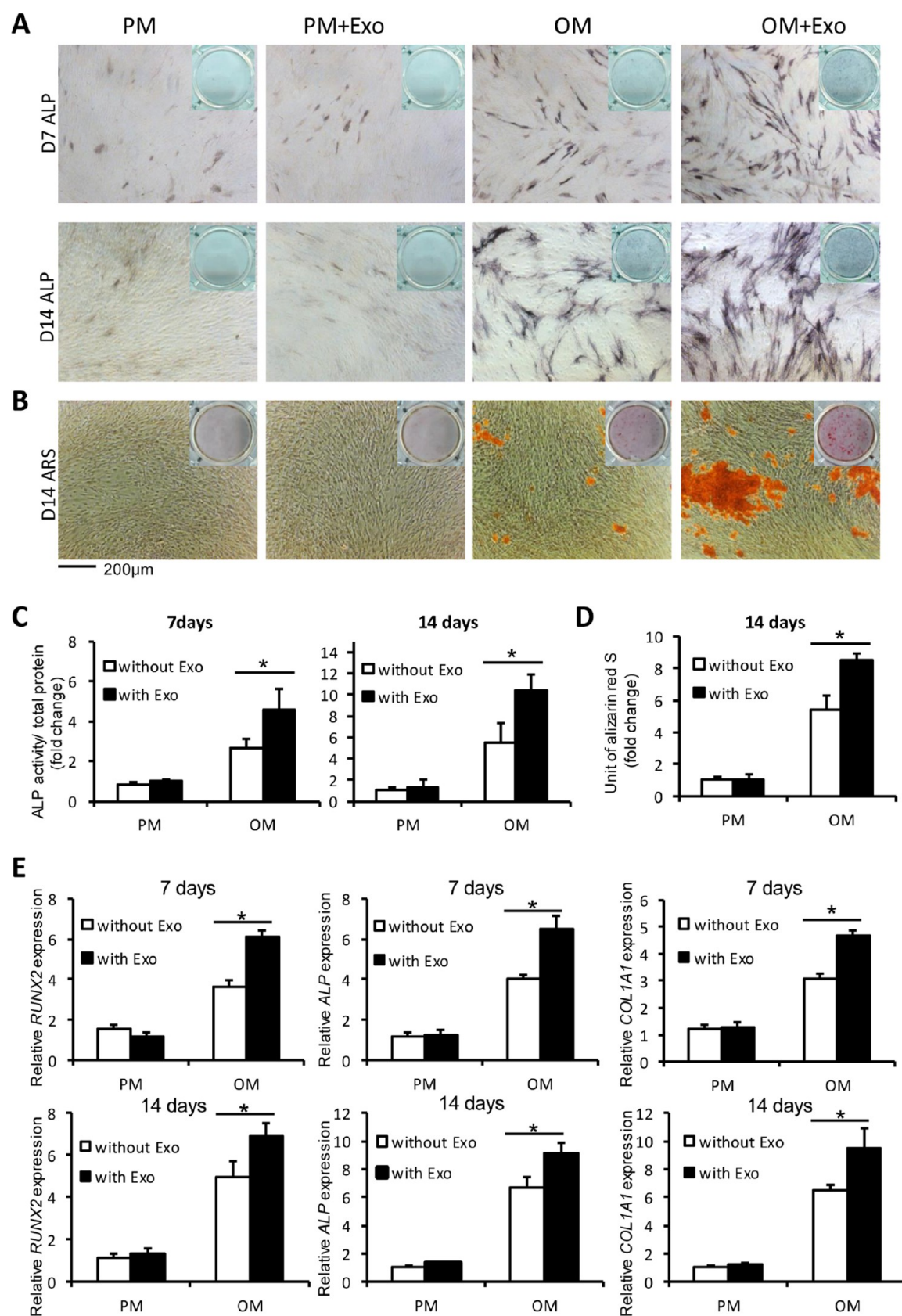
Figure 5. Human adipose-derived stem cells (hASC)-derived exosomes promoted osteogenic differentiation of human bone marrow-derived mesenchymal stem cells (hBMSCs) in vitro. hBMSCs cultured in PM or OM were treated with or without exosomes stained for ALP (A) and alizarin red (B). Quantification of ALP activity (C) and alizarin red (D) of hBMSCs treated with or without exosomes. Expression of osteogenic genes *RUNX2*, *ALP*, and *COL1A1* in hBMSCs cultured with or without exosomes for 7 and 14 days after osteoinduction (E). PM: proliferation medium; OM: osteogenic medium; $*p < 0.05$ compared with the control group.
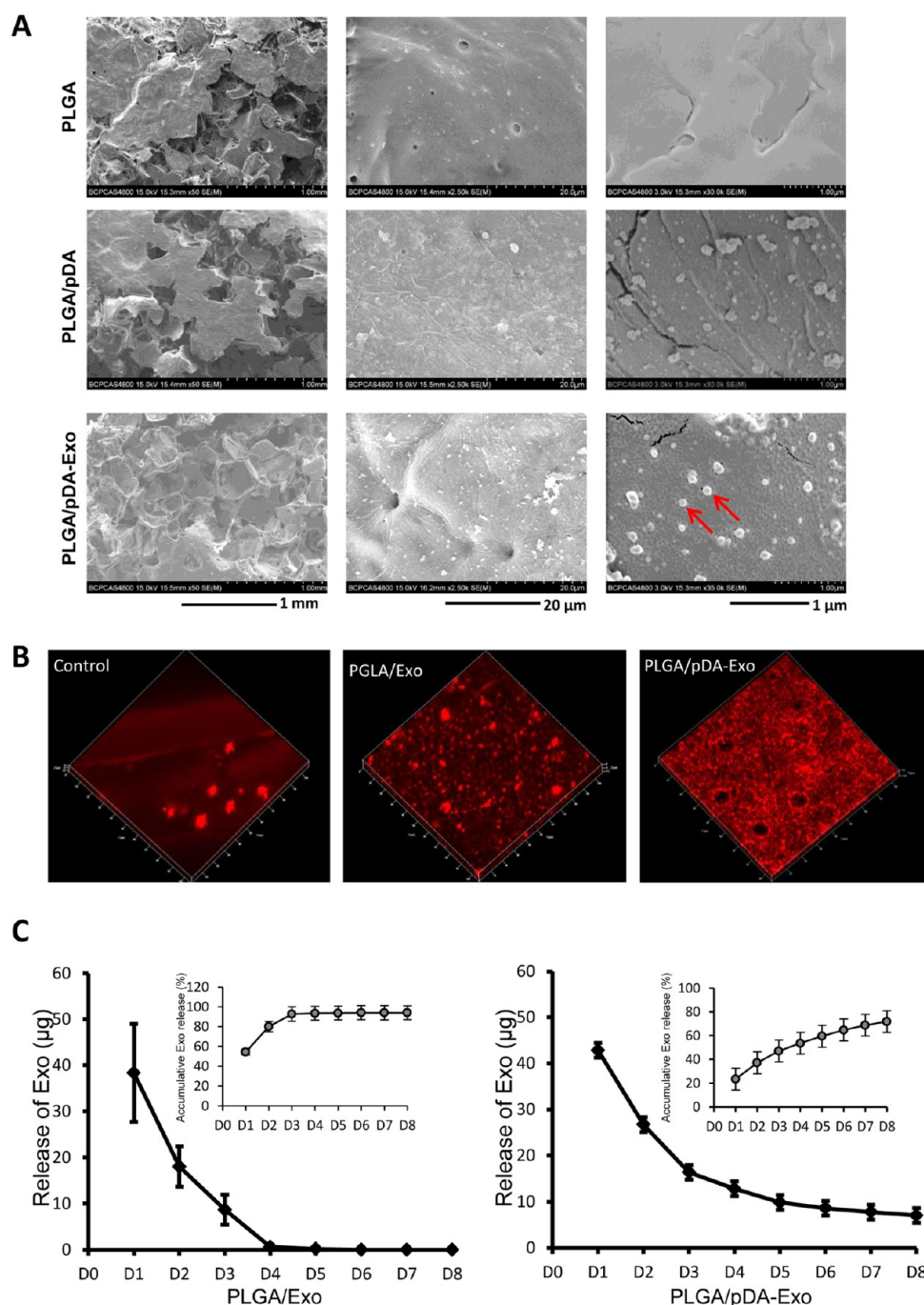
Figure 6. Surface characterization of engineered PLGA substrates. (A) Scanning electron microscopy of PLGA scaffolds (PLGA), PLGA scaffolds coated with polydopamine coating (PLGA/pDA), and PLGA scaffolds coated with polydopamine and exosomes (PLGA/pDA-Exo). (B) Distribution of PKH-26 labeled exosomes on the PLGA-only scaffold (middle) and PLGA/pDA scaffold (right), with PKH-26-stained scaffold as control (left). (C) In vitro exosome release kinetics in saline from exosomes-loaded PLGA by physical absorption (PLGA/Exo) and PLGA/pDA-Exo scaffolds.

regeneration in animal studies,[39,44,45] the potential contamination of undifferentiated tumorigenic iPSCs in iPSC-MSCs may raise the concerns of the safety of iPSC-MSC-Exosomes. As a viable option, hASCs can be highly attractive parent cells due to their easier accessibility, larger availability, lower donor site morbidity, and minimal needs of invasive surgery than that of other MSCs.[46] HASC-derived exosomes have already been shown to significantly alleviate pathology of neurodegenerative diseases by reducing mitochondrial dysfunction[47,48] and promote cutaneous wound healing via optimizing the character-

istics of fibroblasts.[14] To our best knowledge, this is the first report to apply osteogenically induced hASC-derived exosomes and their based TEB to promote the in vitro osteoblastogenesis of hBMSCs and to repair orthotropic bone defects.

The promoting effect of MSC-derived exosomes on osteogenesis is largely attributed to four major mechanisms: (1) protective effect to reduce apoptosis in ischemic and necrotic microenvironments;[42,43] (2) chemotactic and proliferative effect to recruit mesenchymal stem cells and promote their proliferation;[45,49] (3) angiogenic effect to promote
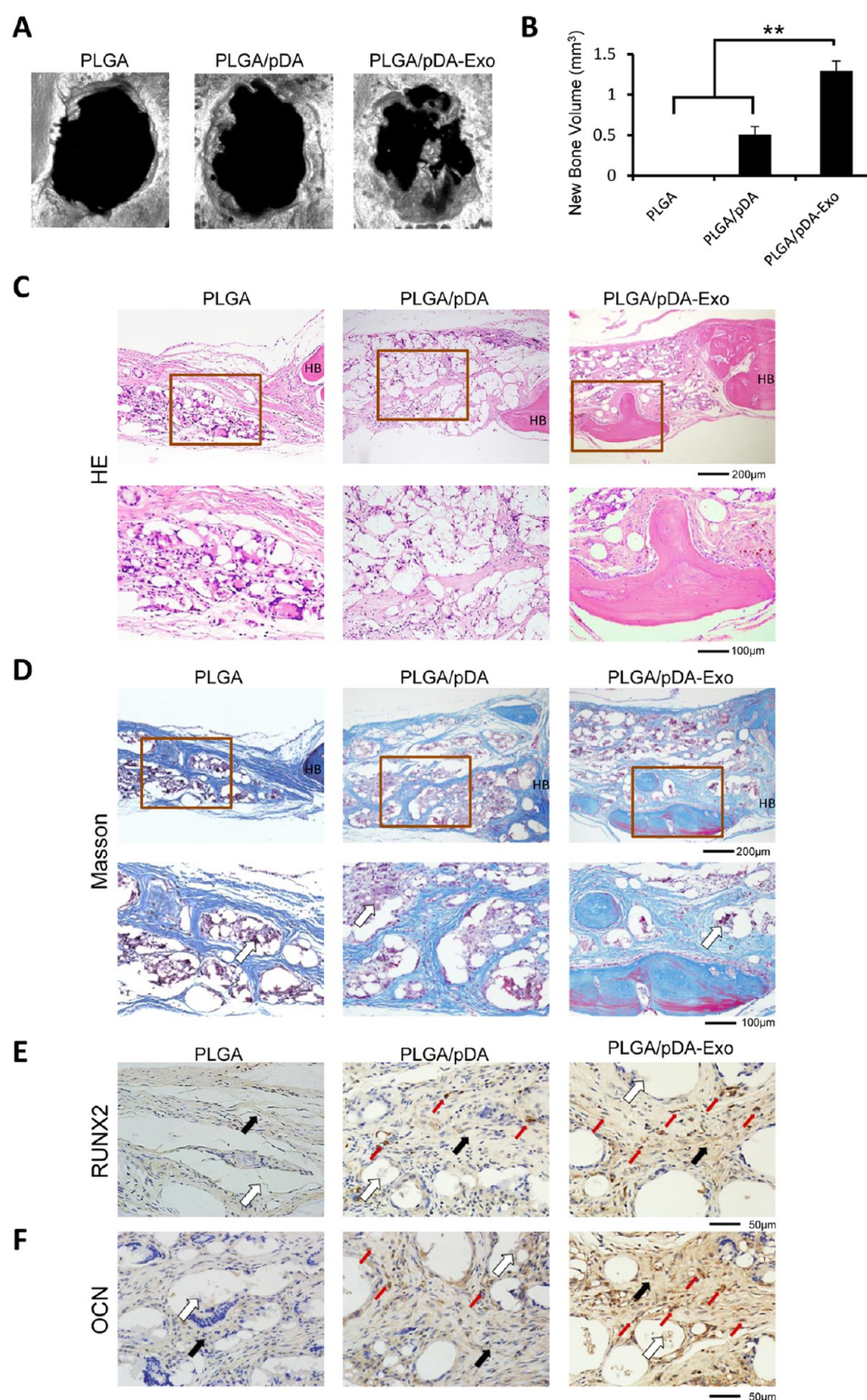
Figure 7. Exosomes increased bone formation in critical-sized mouse calvarial defects. Mice were treated with PLGA scaffolds (PLGA), PLGA scaffolds with polydopamine coating (PLGA/pDA), or PLGA scaffolds coated with polydopamine and exosomes (PLGA/pDA-Exo). (A) Micro-CT images of bone formation in each group after 6 weeks. (B) Quantitative comparison of new bone volume among the different groups. **$p < 0.01$ compared with groups without exosomes. Histological assessment of bone formation in each group: (C) HE staining. (D) Masson staining. The collagen in the bone matrix was stained blue-green. The purple inclusions indicated by the white arrows were the remaining PLGA material. HB, host bone. Immunohistochemical staining for the osteogenic markers (E) RUNX2 and (F) osteocalcin (OCN). Dark-brown granules indicating positive staining are marked by red arrows. The black arrows marked the newly formed tissue and white arrows indicated the area where the remaining PLGA material was located.

vascularization;[41] and (4) osteoinductive effect to directly promote the osteogenic differentiation of MSCs.[41] The first three mechanisms of exosomes appear to derive from the intrinsic functions of their parent cells, MSCs. The fourth mechanism, the osteoinductive effect, is highly needed when hASC-exosomes are applied for bone tissue engineering. In our
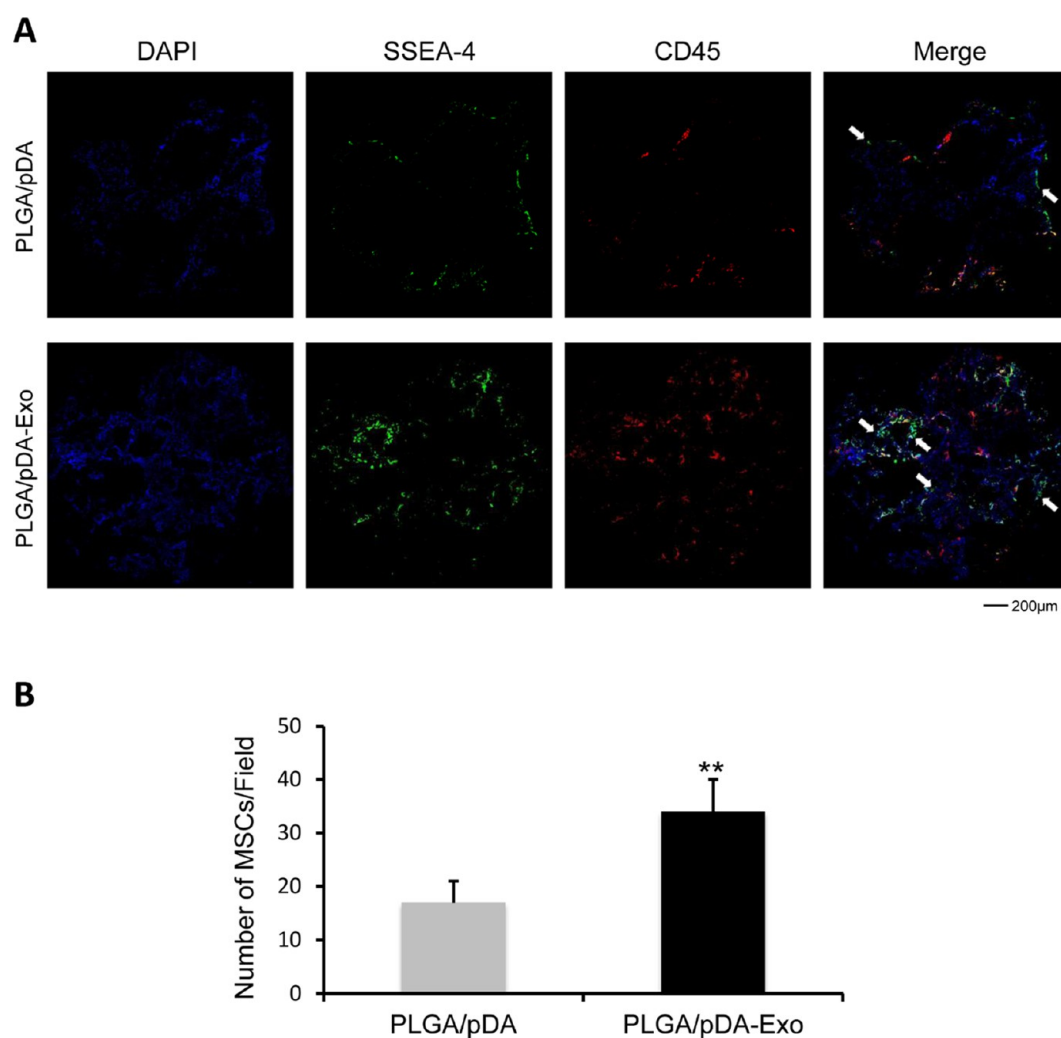
Figure 8. Immunofluorescence staining showed that PLGA scaffolds coated with polydopamine and exosomes (PLGA/pDA-Exo) recruited more SSEA-4$^+$/CD45$^-$ mesenchymal stem cells (MSCs) (indicated by white arrows) than PLGA scaffolds coated with polydopamine (PLGA/pDA) in vivo after 1 week of implantation. (A) Immunofluorescence staining of the two groups. (B) Quantitative analysis of the number of recruited MSCs. **$p < 0.01$ compared with PLGA/pDA group.

study, irrespective of osteogenic induction, hASC-exosomes did not show a significant effect in elevating ALP activity in PM, which indicated that hASC-exosomes even derived from osteogenically induced cells were not sufficient to induce the in vitro osteogenic phenotypic changes of hBMSCs in the level of proteineous markers. One recent study indicated that hASCs and hBMSCs secreted exosomes enriched in distinctive miRNA and tRNA species, which suggested that the tissue-specific microenvironment might influence the exosomal sorting of the MSCs.[50] Martins et al. investigated the osteoinductive effect of the exosomes derived from osteogenically induced BMSCs by either culturing in OM as in this study or by RUNX2 cationic-lipid transfection.[37] Both exosomes could result in a significantly higher ALP activity in the recipient hBMSCs cells cultured in PM only on the 1st day but not in the subsequent 7-day monitoring span.[37] These findings suggested that the exosomes alone could promote but not sufficiently induce the complete in vitro osteoblastogenesis of hBMSCs irrespective of their parent cell type or osteogenic induction. Our finding showed that the osteogenic induction of the parent hASCs significantly enhanced the osteoinductive capacity of their derived exosomes (Figure 3). Such an effect had already

reached a plateau after a 2 day osteogenic induction, and a longer induction did not further enhance the osteoinductive capacity of exosomes. This finding suggested all of the osteoinductive elements had been entrapped into the exosomes only after a 2 day induction, which enables a shortening of the production process of using hASCs to produce osteoinductive exosomes. Twenty five micrograms per milliliter hASC-exosomes were found to be the optimal concentration. In contrast, 100/200 μg/mL or $0.5/1 \times 10^{12}$ particles/mL iPSC-MSC-exosomes have been applied to significantly promote the in vitro osteoblastogenesis of BMSCs.[41,45] The discrepancy in dosage might be due to the difference in phenotype of cells.

Because the functions of exosomes are largely dependent on the phenotypic status of their parent cells, concerns may be raised on whether the intrinsic MSC-derived effects can be compromised by the osteogenic induction. In our result, with the increased osteoinductive effect, the exosomes derived from the 2 day osteogenically induced hASCs could still promote the chemotactic migration by approximately 3-fold and significantly enhance the proliferation of hBMSCs (Figure 4). This finding indicated that the 2 day osteogenic induction did not cause the nullification of the chemotactic and proliferative effects of

exosomes. Thereafter, we showed that the 2 day osteogenically induced hASC-exosomes significantly promoted the osteoblastogenesis of hBMSCs by enhancing ALP activity, extracellular mineralization nodules, and the mRNA expression of the osteoblastogenesis-related genes, such as *RUNX2*, *ALP*, and *COL1A*1 (Figure 5).

Concerns may be raised on the short exosome collection period (2 days) because a prolonged period will definitely yield more exosomes. Our reasoning to choose the 2 days is based on the following three aspects: (1) timeliness for bone repair, (2) yielding of exosomes, and (3) proliferative/chemotactic effects of MSCs exosomes. Our final goal in this study is to develop a clinically applicable and efficacious exosome-based TEB to repair bone defects. When patients get bone defects, they certainly wish to have the defect repaired as soon as possible. Surgeons can achieve ASCs from patients, extract exosomes, and make a cell-free TEB to repair the bone defects. For this purpose, a shorter period to achieve exosomes can provide a very good timeliness for such demands of the patients. Furthermore, MSCs could yield at least 10 times more exosomes than differentiated cells[18] and the EV production might be decreased in confluent cell culture.[51] With the culture process, cells will soon encounter contact inhibition, which may decrease EV secretion and/or alter their characteristics compared to those of actively dividing cells.[52,53] In our study, the osteoinductive effect of exosomes did not become higher in the later time points. However, with the differentiation process, the yielding of exosomes may significantly decrease. Furthermore, the isolation of exosomes is still costly. As we discussed above, the proliferative and chemotactic effects of transplanted MSCs on host MSCs are one of the most important mechanisms to promote bone regeneration. In our study, we also showed that the exosomes derived from 2 day osteogenically induced ASCs still bore strong proliferative and chemotactic effects (Figure 4). Although we did not prove it, there might be a trend that such proliferative and chemotactic effects of exosomes taper at later time points because the cells would soon lose their MSC properties. Considering all of the above mentioned points, a 2 day collection period might be one good time point for achieving the optimal property of exosomes. However, this view should be further experimentally clarified.

The mechanism underlying the biological effect of exosomes seems to be the transfer of mRNA, miRNA, and proteins.[35,54] MicroRNAs are post-transcriptional regulators that could influence bone formation and bone remodeling by networking with cell signaling pathways and intricating transcriptional programs.[55] Our previous studies have indicated that several miRNAs, like miR-34a, could modulate the osteogenesis of hASCs.[56] The miRNA expression profile in exosomes altered during the osteogenic differentiation.[57] Some osteogenesis-related miRNAs, such as let-7a and miR-218, were up- or downregulated at different time points, and the alteration was helpful to the osteogenic differentiation of MSCs. In addition to small RNA, Zhang et al. showed that the exosomes derived from iPSC-MSCs without osteogenic induction could enhance the osteogenic differentiation of hBMSCs by activating the PI3K/Akt signaling pathway.[45] Hitherto, no reports have been performed to uncover the mechanisms accounting for the osteoinductive effect of osteogenically induced hASC-derived exosomes. The precise mechanism needs to be further investigated.

It is well recognized that in the process of bone repair and regeneration, endogenous MSCs can be chemotactically recruited to the injury site and function as the major healing cells.[58] Locally applied exosomes are also expected to exert the functions as growth factor or cytokines to promote the chemotactic homing, proliferation, and osteogenic differentiation of MSCs. A local and slow-release pattern should also be achieved to ensure the sufficient duration of their functions.[41] Consequently, an ideal scaffold for exosome-based tissue engineering should be biocompatible, biodegradable, and capable of releasing exosomes in a controlled and slow manner. Such scaffolds should also provide temporary physical support before the neobone tissue takes over.[59] PLGA is widely recognized as a biocompatible and biodegradable biomaterial and has already been widely used as a biomedical material in clinics.[60] However, there is still lack of capacity of slow-releasing bioactive agents for PLGA. In our previous study, we successfully used a mussel-inspired immobilization strategy mediated by pDA to introduce osteoinductive peptides onto the surface of PLGA substrate to overcome these challenges.[28] pDA has been widely used in the fields of biomaterials and bone tissue engineering to modify the surface characteristics of scaffolds. This material is highly commendable for cytocompatibility, biocompatibility, and biodegradability for biomedical application.[6] The most invaluable property is that pDA is highly adhesive for biological reagents. This property is widely applied for anchoring synthetic and biological substances onto various substrates for biomedical applications.[61] In our previous study, we showed that the pDA-mediated surface modification could slow the degradation of PLGA (50/50) to a rate that was suitable for bone formation, whereas the scaffolds without modification were completely absorbed 8 weeks after implantation.[28,62] In this study, we, for the first time, applied pDA to adhere, carry, and retain exosomes so as to enable a slow and local release profile of exosomes. About 165.72 ± 15.4 μg of exosomes per scaffold could be incorporated on each PLGA/pDA scaffold. Furthermore, our in vitro release study showed that about $28.19 \pm 9.2\%$ exosomes were still retained in the scaffold after 8 days (Figure 6). In contrast, superficial adsorption was associated with a significantly lower loading (about 73.6 ± 22.4 μg) than that of the PLGA/pDA scaffold. Consistent with a previous study,[45] these exosomes were almost completely depleted within 4 days when exosomes were directly adsorbed onto materials (Figure 6C). These findings indicated that the pDA surface was a convenient, viable, and efficient carrier for the slow release of exosomes, which is very promising for the application in exosome-based tissue engineering.

Consistent with the in vitro finding, micro-CT and histological analyses revealed that the addition of the exosomes resulted in significantly more new bone tissue than that in the control group (without exosomes) in the in vivo critical-sized bone defects (Figure 7). To further explore the possible mechanisms of bone formation in the TEB, we studied MSC homing. According to our previous study, we detected SSEA-4$^+$/CD45$^-$ MSCs in the scaffold implanted into the calvarial defect area one week after the surgery (Figure 8). As the TEB was a cell-free system, the MSCs appearing in the scaffolds were assumed to come from surrounding MSC resources or circulation. Consistent with the in vitro experiments, we found that the number of MSCs recruited in the presence of exosomes was about 2-fold compared with that without exosomes. In bone tissue regeneration, the essential roles of

MSCs are well recognized.[6] Therefore, the effect of exosomes on MSC recruitment may be one mechanism for the improved bone regeneration in critical-sized calvarial defects. The promoting effect of the 2 day osteogenically induced hASC-exosomes on the osteogenic differentiation of host MSCs in vivo was corroborated by the significantly higher number of RUNX2- and OCN-positive cells (Figure 7E,F), which is consistent with the previous studies.[45] Collectively, these results largely satisfy the conditions of successful tissue engineering bone and can be applied for enhanced bone regeneration.

There still existed some limitations about our study. First, the evaluation of bone formation in vivo could be performed at additional time points. Second, the mechanism behind the exosomes' effect is not clearly defined and needed further exploration on the basis of our current study.

CONCLUSIONS

Exosomes derived from hASCs enhance the migration, proliferation, and osteogenic differentiation of hBMSCs in vitro, and the cell-free bone tissue engineering system combining PLGA/pDA scaffolds with exosomes promotes bone regeneration in mouse critical-sized calvarial defects.

ASSOCIATED CONTENT

Ⓢ Supporting Information

The Supporting Information is available free of charge on the ACS Publications website at DOI: 10.1021/acsami.7b17620.

ALP staining and activity assay, Alizarin red S staining and gene expression confirmed the osteogenic differentiation of hASCs (PDF)

AUTHOR INFORMATION

Corresponding Authors
*E-mail: zx8213163@163.com. Tel: +86 10 82195321 (X.Z.).
*E-mail: g.wu@acta.nl. Tel: +31 20 598 0866 (G.W.).
*E-mail: kqzhouysh@hsc.pku.edu.cn. Tel: +86 10 82195370 (Y.Z.).
ORCID Ⓘ
Yongsheng Zhou: 0000-0002-4332-0878
Notes
The authors declare no competing financial interest.

ACKNOWLEDGMENTS

REFERENCES

(1) Huey, D. J.; Hu, J. C.; Athanasiou, K. A. Unlike Bone, Cartilage Regeneration Remains Elusive. *Science* 2012, 338, 917−921.
(2) Bianco, P.; Cao, X.; Frenette, P. S.; Mao, J. J.; Robey, P. G.; Simmons, P. J.; Wang, C.-Y. The Meaning, the Sense and the Significance: Translating the Science of Mesenchymal Stem Cells into Medicine. *Nat. Med.* 2013, 19, 35−42.
(3) Fennema, E. M.; Tchang, L. A. H.; Yuan, H.; van Blitterswijk, C. A.; Martin, I.; Scherberich, A.; de Boer, J. Ectopic Bone Formation by Aggregated Mesenchymal Stem Cells from Bone Marrow and Adipose Tissue: A Comparative Study. *J. Tissue Eng. Regener. Med.* 2017, 12, e150−e158.

(4) Kanelidis, A. J.; Premer, C.; Lopez, J.; Balkan, W.; Hare, J. M. Route of Delivery Modulates the Efficacy of Mesenchymal Stem Cell Therapy for Myocardial Infarction: A Meta-Analysis of Preclinical Studies and Clinical Trials. *Circ. Res.* 2017, 120, 1139−1150.
(5) Vega, A.; Martín-Ferrero, M. A.; Del Canto, F.; Alberca, M.; García, V.; Munar, A.; Orozco, L.; Soler, R.; Fuertes, J. J.; Huguet, M.; Sánchez, A.; García-Sancho, J. Treatment of Knee Osteoarthritis With Allogeneic Bone Marrow Mesenchymal Stem Cells: A Randomized Controlled Trial. *Transplantation* 2015, 99, 1681−1690.
(6) Liu, Y. S.; Ou, M. E.; Liu, H.; Gu, M.; Lv, L. W.; Fan, C.; Chen, T.; Zhao, X. H.; Jin, C. Y.; Zhang, X.; Ding, Y.; Zhou, Y. S. The Effect of Simvastatin on Chemotactic Capability of SDF-1alpha and the Promotion of Bone Regeneration. *Biomaterials* 2014, 35, 4489−4498.
(7) Eggenhofer, E.; Luk, F.; Dahlke, M. H.; Hoogduijn, M. J. The Life and Fate of Mesenchymal Stem Cells. *Front. Immunol.* 2014, 5, No. 148.
(8) Caplan, A. I.; Correa, D. The MSC: An Injury Drugstore. *Cell Stem Cell* 2011, 9, 11−15.
(9) Gnecchi, M.; He, H.; Liang, O. D.; Melo, L. G.; Morello, F.; Mu, H.; Noiseux, N.; Zhang, L.; Pratt, R. E.; Ingwall, J. S.; Dzau, V. J. Paracrine Action Accounts for Marked Protection of Ischemic Heart by Akt-modified Mesenchymal Stem Cells. *Nat. Med.* 2005, 11, 367−368.
(10) Timmers, L.; Lim, S. K.; Arslan, F.; Armstrong, J. S.; Hoefer, I. E.; Doevendans, P. A.; Piek, J. J.; El Oakley, R. M.; Choo, A.; Lee, C. N.; Pasterkamp, G.; de Kleijn, D. P. Reduction of Myocardial Infarct Size by Human Mesenchymal Stem Cell Conditioned Medium. *Stem Cell Res.* 2007, 1, 129−137.
(11) Milane, L.; Singh, A.; Mattheolabakis, G.; Suresh, M.; Amiji, M. M. Exosome Mediated Communication within the Tumor Microenvironment. *J. Controlled Release* 2015, 219, 278−294.
(12) Melo, S. A.; Sugimoto, H.; O'Connell, J. T.; Kato, N.; Villanueva, A.; Vidal, A.; Qiu, L.; Vitkin, E.; Perelman, L. T.; Melo, C. A.; Lucci, A.; Ivan, C.; Calin, G. A.; Kalluri, R. Cancer Exosomes Perform Cell-Independent microRNA Biogenesis and Promote Tumorigenesis. *Cancer Cell* 2014, 26, 707−721.
(13) Melo, S. A.; Luecke, L. B.; Kahlert, C.; Fernandez, A. F.; Gammon, S. T.; Kaye, J.; LeBleu, V. S.; Mittendorf, E. A.; Weitz, J.; Rahbari, N.; Reissfelder, C.; Pilarsky, C.; Fraga, M. F.; Piwnica-Worms, D.; Kalluri, R. Glypican-1 Identifies Cancer Exosomes and Detects Early Pancreatic Cancer. *Nature* 2015, 523, 177−182.
(14) Hu, L.; Wang, J.; Zhou, X.; Xiong, Z.; Zhao, J.; Yu, R.; Huang, F.; Zhang, H.; Chen, L. Exosomes Derived from Human Adipose Mensenchymal Stem Cells Accelerates Cutaneous Wound Healing via Optimizing the Characteristics of Fibroblasts. *Sci. Rep.* 2016, 6, No. 32993.
(15) Kaur, S.; Singh, S. P.; Elkahloun, A. G.; Wu, W.; Abu-Asab, M. S.; Roberts, D. D. CD47-Dependent Immunomodulatory and Angiogenic Activities of Extracellular Vesicles Produced by T Cells. *Matrix Biol.* 2014, 37, 49−59.
(16) Soldevilla, B.; Rodríguez, M.; San Millán, C.; García, V.; Fernández-Periañez, R.; Gil-Calderón, B.; Martín, P.; García-Grande, A.; Silva, J.; Bonilla, F.; Domínguez, G. Tumor-Derived Exosomes Are Enriched in ΔNp73, which Promotes Oncogenic Potential in Acceptor Cells and Correlates with Patient Survival. *Hum. Mol. Genet.* 2014, 23, 467−478.
(17) Kosaka, N.; Iguchi, H.; Hagiwara, K.; Yoshioka, Y.; Takeshita, F.; Ochiya, T. Neutral Sphingomyelinase 2 (nSMase2)-Dependent Exosomal Transfer of Angiogenic MicroRNAs Regulate Cancer Cell Metastasis. *J. Biol. Chem.* 2013, 288, 10849−10859.
(18) Yeo, R. W.; Lai, R. C.; Zhang, B.; Tan, S. S.; Yin, Y.; Teh, B. J.; Lim, S. K. Mesenchymal Stem Cell: An Efficient Mass Producer of Exosomes for Drug Delivery. *Adv. Drug Delivery Rev.* 2013, 65, 336−341.
(19) Liu, S.; Liu, D.; Chen, C.; Hamamura, K.; Moshaverinia, A.; Yang, R.; Liu, Y.; Jin, Y.; Shi, S. MSC Transplantation Improves Osteopenia via Epigenetic Regulation of Notch Signaling in Lupus. *Cell Metab.* 2015, 22, 606−618.

(20) Nakano, M.; Nagaishi, K.; Konari, N.; Saito, Y.; Chikenji, T.; Mizue, Y.; Fujimiya, M. Bone Marrow-Derived Mesenchymal Stem Cells Improve Diabetes-Induced Cognitive Impairment by Exosome Transfer into Damaged Neurons and Astrocytes. *Sci. Rep.* **2016**, *6*, No. 24805.

(21) Sahoo, S.; Losordo, D. W. Exosomes and Cardiac Repair after Myocardial Infarction. *Circ. Res.* **2014**, *114*, 333–344.

(22) Andaloussi, S. E.; Lakhal, S.; Mager, I.; Wood, M. J. Exosomes for Targeted siRNA Delivery Across Biological Barriers. *Adv. Drug Delivery Rev.* **2013**, *65*, 391–397.

(23) Rada, T.; Reis, R. L.; Gomes, M. E. Adipose Tissue-Derived Stem Cells and Their Application in Bone and Cartilage Tissue Engineering. *Tissue Eng., Part B* **2009**, *15*, 113–125.

(24) Zhang, X.; Guo, J.; Wu, G.; Zhou, Y. Effects of Heterodimeric Bone Morphogenetic Protein-2/7 on Osteogenesis of Human Adipose-Derived Stem Cells. *Cell Proliferation* **2015**, *48*, 650–660.

(25) Togliatto, G.; Dentelli, P.; Gili, M.; Gallo, S.; Deregibus, C.; Biglieri, E.; Iavello, A.; Santini, E.; Rossi, C.; Solini, A.; Camussi, G.; Brizzi, M. F. Obesity Reduces the Pro-Angiogenic Potential of Adipose Tissue Stem Cell-Derived Extracellular Vesicles (EVs) by Impairing miR-126 Content: Impact on Clinical Applications. *Int. J. Obes.* **2016**, *40*, 102–111.

(26) Luo, L.; Tang, J.; Nishi, K.; Yan, C.; Dinh, P. U.; Cores, J.; Kudo, T.; Zhang, J.; Li, T. S.; Cheng, K. Fabrication of Synthetic Mesenchymal Stem Cells for the Treatment of Acute Myocardial Infarction in Mice. *Circ. Res.* **2017**, *120*, 1768–1775.

(27) Lee, Y. J.; Lee, J. H.; Cho, H. J.; Kim, H. K.; Yoon, T. R.; Shin, H. Electrospun Fibers Immobilized With Bone Forming Peptide-1 Derived from BMP7 for Guided Bone Regeneration. *Biomaterials* **2013**, *34*, 5059–5069.

(28) Li, W.; Zheng, Y.; Zhao, X.; Ge, Y.; Chen, T.; Liu, Y.; Zhou, Y. Osteoinductive Effects of Free and Immobilized Bone Forming Peptide-1 on Human Adipose-Derived Stem Cells. *PloS One* **2016**, *11*, No. e0150294.

(29) Bang, C.; Batkai, S.; Dangwal, S.; Gupta, S. K.; Foinquinos, A.; Holzmann, A.; Just, A.; Remke, J.; Zimmer, K.; Zeug, A.; Ponimaskin, E.; Schmiedl, A.; Yin, X.; Mayr, M.; Halder, R.; Fischer, A.; Engelhardt, S.; Wei, Y.; Schober, A.; Fiedler, J.; Thum, T. Cardiac Fibroblast-Derived MicroRNA Passenger Strand-Enriched Exosomes Mediate Cardiomyocyte Hypertrophy. *J. Clin. Invest.* **2014**, *124*, 2136–2146.

(30) Théry, C.; Amigorena, S.; Raposo, G.; Clayton, A. Isolation and Characterization of Exosomes from Cell Culture Supernatants and Biological Fluids. In *Current Protocols in Cell Biology*; Wiley, 2006; Chapter 3, pp 3.22.1–3.22.29.

(31) Song, X.; Ding, Y.; Liu, G.; Yang, X.; Zhao, R.; Zhang, Y.; Zhao, X.; Anderson, G. J.; Nie, G. Cancer Cell-Derived Exosomes Induce Mitogen-Activated Protein Kinase-Dependent Monocyte Survival by Transport of Functional Receptor Tyrosine Kinases. *J. Biol. Chem.* **2016**, *291*, 8453–8464.

(32) Lötvall, J.; Hill, A. F.; Hochberg, F.; Buzas, E. I.; Di Vizio, D.; Gardiner, C.; Gho, Y. S.; Kurochkin, I. V.; Mathivanan, S.; Quesenberry, P.; Sahoo, S.; Tahara, H.; Wauben, M. H.; Witwer, K. W.; Thery, C. Minimal Experimental Requirements for Definition of Extracellular Vesicles and Their Functions: A Position Statement from the International Society for Extracellular Vesicles. *J. Extracell. Vesicles* **2014**, *3*, No. 26913.

(33) Thevenot, P. T.; Nair, A. M.; Shen, J.; Lotfi, P.; Ko, C.-Y.; Tang, L. The Effect of Incorporation of SDF-1α into PLGA Scaffolds on Stem Cell Recruitment and the Inflammatory Response. *Biomaterials* **2010**, *31*, 3997–4008.

(34) Qazi, T. H.; Mooney, D. J.; Pumberger, M.; Geißler, S.; Duda, G. N. Biomaterials Based Strategies for Skeletal Muscle Tissue Engineering: Existing Technologies and Future Trends. *Biomaterials* **2015**, *53*, 502–521.

(35) Tassetto, M.; Kunitomi, M.; Andino, R. Circulating Immune Cells Mediate a Systemic RNAi-Based Adaptive Antiviral Response in Drosophila. *Cell* **2017**, *169*, 314.

(36) Qin, Y.; Wang, L.; Gao, Z.; Chen, G.; Zhang, C. Bone Marrow Stromal/Stem Cell-Derived Extracellular Vesicles Regulate Osteoblast Activity and Differentiation in Vitro and Promote Bone Regeneration in Vivo. *Sci. Rep.* **2016**, *6*, No. 21961.

(37) Martins, M.; Ribeiro, D.; Martins, A.; Reis, R. L.; Neves, N. M. Extracellular Vesicles Derived from Osteogenically Induced Human Bone Marrow Mesenchymal Stem Cells Can Modulate Lineage Commitment. *Stem Cell Rep.* **2016**, *6*, 284–291.

(38) Ekström, K.; Omar, O.; Graneli, C.; Wang, X.; Vazirisani, F.; Thomsen, P. Monocyte Exosomes Stimulate the Osteogenic Gene Expression of Mesenchymal Stem Cells. *PLoS One* **2013**, *8*, No. e75227.

(39) Villa-Diaz, L. G.; Brown, S. E.; Liu, Y.; Ross, A. M.; Lahann, J.; Parent, J. M.; Krebsbach, P. H. Derivation of Mesenchymal Stem Cells from Human Induced Pluripotent Stem Cells Cultured on Synthetic Substrates. *Stem Cells* **2012**, *30*, 1174–1181.

(40) Herberts, C. A.; Kwa, M. S.; Hermsen, H. P. Risk Factors in the Development of Stem Cell Therapy. *J. Transl. Med.* **2011**, *9*, No. 29.

(41) Qi, X.; Zhang, J.; Yuan, H.; Xu, Z.; Li, Q.; Niu, X.; Hu, B.; Wang, Y.; Li, X. Exosomes Secreted by Human-Induced Pluripotent Stem Cell-Derived Mesenchymal Stem Cells Repair Critical-Sized Bone Defects through Enhanced Angiogenesis and Osteogenesis in Osteoporotic Rats. *Int. J. Biol. Sci.* **2016**, *12*, 836–849.

(42) Hu, G. W.; Li, Q.; Niu, X.; Hu, B.; Liu, J.; Zhou, S. M.; Guo, S. C.; Lang, H. L.; Zhang, C. Q.; Wang, Y.; Deng, Z. F. Exosomes Secreted by Human-Induced Pluripotent Stem Cell-Derived Mesenchymal Stem Cells Attenuate Limb Ischemia by Promoting Angiogenesis in Mice. *Stem Cell Res. Ther.* **2015**, *6*, No. 10.

(43) Liu, X.; Li, Q.; Niu, X.; Hu, B.; Chen, S.; Song, W.; Ding, J.; Zhang, C.; Wang, Y. Exosomes Secreted from Human-Induced Pluripotent Stem Cell-Derived Mesenchymal Stem Cells Prevent Osteonecrosis of the Femoral Head by Promoting Angiogenesis. *Int. J. Biol. Sci.* **2017**, *13*, 232–244.

(44) Zou, L.; Luo, Y.; Chen, M.; Wang, G.; Ding, M.; Petersen, C. C.; Kang, R.; Dagnaes-Hansen, F.; Zeng, Y.; Lv, N.; Ma, Q.; Le, D. Q.; Besenbacher, F.; Bolund, L.; Jensen, T. G.; Kjems, J.; Pu, W. T.; Bunger, C. A Simple Method for Deriving Functional MSCs and Applied for Osteogenesis in 3D Scaffolds. *Sci. Rep.* **2013**, *3*, No. 2243.

(45) Zhang, J.; Liu, X. L.; Li, H. Y.; Chen, C. Y.; Hu, B.; Niu, X.; Li, Q.; Zhao, B. Z.; Xie, Z. P.; Wang, Y. Exosomes/Tricalcium Phosphate Combination Scaffolds Can Enhance Bone Regeneration by Activating the PI3K/Akt Signaling Pathway. *Stem Cell Res. Ther.* **2016**, *7*, No. 136.

(46) Levi, B.; Longaker, M. T. Concise Review: Adipose-Derived Stromal Cells for Skeletal Regenerative Medicine. *Stem Cells* **2011**, *29*, 576–582.

(47) Lee, M.; Ban, J. J.; Kim, K. Y.; Jeon, G. S.; Im, W.; Sung, J. J.; Kim, M. Adipose-Derived Stem Cell Exosomes Alleviate Pathology of Amyotrophic Lateral Sclerosis in Vitro. *Biochem. Biophys. Res. Commun.* **2016**, *479*, 434–439.

(48) Lee, M.; Liu, T.; Im, W.; Kim, M. Exosomes from Adipose-Derived Stem Cells Ameliorate Phenotype of Huntington's Disease in Vitro Model. *Eur. J. Neurosci.* **2016**, *44*, 2114–2119.

(49) Furuta, T.; Miyaki, S.; Ishitobi, H.; Ogura, T.; Kato, Y.; Kamei, N.; Miyado, K.; Higashi, Y.; Ochi, M. Mesenchymal Stem Cell-Derived Exosomes Promote Fracture Healing in A Mouse Model. *Stem Cells Transl. Med.* **2016**, *5*, 1620–1630.

(50) Baglio, S. R.; Rooijers, K.; Koppers-Lalic, D.; Verweij, F. J.; Perez Lanzon, M.; Zini, N.; Naaijkens, B.; Perut, F.; Niessen, H. W.; Baldini, N.; Pegtel, D. M. Human Bone Marrow- and Adipose-Mesenchymal Stem Cells Secrete Exosomes Enriched in Distinctive miRNA and tRNA Species. *Stem Cell Res. Ther.* **2015**, *6*, No. 127.

(51) Gudbergsson, J. M.; Johnsen, K. B.; Skov, M. N.; Duroux, M. Systematic Review of Factors Influencing Extracellular Vesicle Yield from Cell Cultures. *Cytotechnology* **2016**, *68*, 579–592.

(52) Steinman, R. A.; Wentzel, A.; Lu, Y.; Stehle, C.; Grandis, J. R. Activation of Stat3 by Cell Confluence Reveals Negative Regulation of Stat3 by cdk2. *Oncogene* **2003**, *22*, 3608–3615.

(53) Hayes, O.; Ramos, B.; Rodriguez, L. L.; Aguilar, A.; Badia, T.; Castro, F. O. Cell Confluency Is as Efficient as Serum Starvation for Inducing Arrest in the G0/G1 Phase of the Cell Cycle in Granulosa and Fibroblast Cells of Cattle. *Anim. Reprod. Sci.* **2005**, *87*, 181–192.

(54) Toh, W. S.; Lai, R. C.; Hui, J. H. P.; Lim, S. K. MSC Exosome as A Cell-Free MSC Therapy for Cartilage Regeneration: Implications for Osteoarthritis Treatment. *Semin. Cell Dev. Biol.* **2017**, *67*, 56−64.

(55) Vimalraj, S.; Selvamurugan, N. MicroRNAs: Synthesis, Gene Regulation and Osteoblast Differentiation. *Curr. Issues Mol. Biol.* **2013**, *15*, 7−18.

(56) Fan, C.; Jia, L.; Zheng, Y.; Jin, C.; Liu, Y.; Liu, H.; Zhou, Y. MiR-34a Promotes Osteogenic Differentiation of Human Adipose-Derived Stem Cells via the RBP2/NOTCH1/CYCLIN D1 Coregulatory Network. *Stem Cell Rep.* **2016**, *7*, 236−248.

(57) Xu, J. F.; Yang, G. H.; Pan, X. H.; Zhang, S. J.; Zhao, C.; Qiu, B. S.; Gu, H. F.; Hong, J. F.; Cao, L.; Chen, Y.; Xia, B.; Bi, Q.; Wang, Y. P. Altered microRNA Expression Profile in Exosomes During Osteogenic Differentiation of Human Bone Marrow-Derived Mesenchymal Stem Cells. *PLoS One* **2014**, *9*, No. e114627.

(58) Wang, X.; Wang, Y.; Gou, W.; Lu, Q.; Peng, J.; Lu, S. Role of Mesenchymal Stem Cells in Bone Regeneration and Fracture Repair: A Review. *Int. Orthop.* **2013**, *37*, 2491−2498.

(59) Zhang, Z.; Hu, J.; Ma, P. X. Nanofiber-based Delivery of Bioactive Agents and Stem Cells to Bone Sites. *Adv. Drug Delivery Rev.* **2012**, *64*, 1129−1141.

(60) Pashuck, E. T.; Stevens, M. M. Designing Regenerative Biomaterial Therapies for the Clinic. *Sci. Transl. Med.* **2012**, *4*, No. 160sr4.

(61) Ho, C. C.; Ding, S. J. Structure, Properties and Applications of Mussel-Inspired Polydopamine. *J. Biomed. Nanotechnol.* **2014**, *10*, 3063−3084.

(62) Lu, L.; Peter, S. J.; Lyman, M. D.; Lai, H. L.; Leite, S. M.; Tamada, J. A.; Uyama, S.; Vacanti, J. P.; Langer, R.; Mikos, A. G. In Vitro and in Vivo Degradation of Porous Poly(dl-Lactic-*co*-Glycolic Acid) Foams. *Biomaterials* **2000**, *21*, 1837−1845.